INVESTIGATION OF HYGROTHERMAL AGEING PHENOMENA IN MODEL COMPOSITES BY RAMAN SPECTROSCOPY

A. J. Cervenka[1], R. J. Young[1] and K. Kueseng[2]

[1] Manchester Materials Science Centre, University of Manchester and UMIST, Manchester M1 7HS, United Kingdom
[2] Institute of Science, Walailak University Thasala, Nakornsrithammarat, 80160 Thailand

ABSTRACT

Raman spectroscopy combined with gravimetry is used to investigate hygrothermal ageing in model composites based on an epoxy resin containing a single filament of a reinforcing fibre. Three fibre types, namely PBO, M5 and Twaron are examined using two specimen configurations - the diffusion slab (DS) and the double fibre pull out (DFPO) geometry. In addition the effect of surface treatment is studied in the case of Twaron fibres: an untreated fibre (HM), a fibre with a surface finish (HMF) and a fibre with an activated surface (HMA). Ageing aspects of the fibres are assessed by monitoring development of the Raman strain profiles $\varepsilon(x,t)$ and the water uptake $M(t)$ with time. Experimental moisture uptakes are modelled using relationships that describe Fickian diffusion into a solid parallelepiped as time dependencies controlled by the specimen geometry, diffusion coefficient of the matrix, D, and the equilibrium uptake of water, $M(\infty)$. Simple micromechanical models facilitate rationalisation of the Raman strain profiles in the terms of the mid-fibre strain $\varepsilon(x=0,t)$, the dimensionless Raman shear-lag parameter n (which controls stress transfer along the interface) and - at longer exposure times when debonding is observed for some fibres – the time evolution of the debond length $L_d(t)$. These time dependencies allow the fibres – and in the case of Twaron also merits of the surface treatment – to be ranked in terms of their relative stability of the fibre/matrix interface. Eliminating the exposure time as a variable, dependence of the corrected mid-fibre strain $\varepsilon(x=0,t) - \varepsilon_0$ on the moisture uptake $M(t)$ yields an information about the swelling aspects. As to the fibres, Twaron HMA has the most durable interface in the ageing epoxy matrix. PBO appears to be worse, with the Twaron HM and HMF fibres between. Unusual behaviour has been found for the M5 fibre

1. INTRODUCTION

An appreciable effort has been invested into development of stiff, strong polymeric fibres for composite reinforcement and modification of their surfaces to warrant the most efficient stress transfer in the fibre/matrix interface. Much lesser work has been done with the aim to understand the behaviour of these fibres during hygrothermal ageing and to assess the interface stability with respect to the ingressing moisture. Fully appreciating that any chance to use polymeric composites in structural applications is inseparable from understanding the micromechanical aspects of composite ageing, we have developed a procedure for studying model composites ageing under a simple laboratory regime. The procedure [1] is based on combination of the Raman spectroscopy and gravimetry supported by theoretical relationships [2] describing three-dimensional diffusion into small orthogonal specimens.

The aim of this communication is to report on application of this procedure to three novel polymeric reinforcements and to assess durability of their interfaces in an epoxy resin. The fibre studied are: Twaron, poly(p-phenylene benzobisoxazole) usually abbreviated as PBO and commercialised under the trade name Zylon® [3] and poly[2,6-diimidazo(4,5-b:4’,5’-e) pyridynylene-1,4(2,5-dihydroxy)phenylene] also known as PIPD (polypyridobisimazole) or, alternatively [4], coded as M5. In addition, the effect of surface treatment on fibre suitability for applications of composites under ‘wet’ conditions has been also studied by examining the behaviour of the Twaron fibre with three types of surface modification: an untreated fibre (HM), the fibre with a surface finish (HMF) and the fibre with an activated surface (HMA).

Conclusions are drawn for three aspects of the ageing process: 1) Predictability of observed $M(t)$ values from the characteristics of the diffusion process – diffusion coefficient D and the equilibrium moisture uptake $M(\infty)$; 2) Stability of the fibre/matrix interface during the exposure to moisture at ambient temperature from the time dependences of the quantities deduced from the Raman spectroscopy – $n(t)$ and $L_d(t)$ and 3) Swelling behaviour of the constituents from the dependencies of the corrected mid-fibre strain $\varepsilon(x=0,t) - \varepsilon_0$ on the moisture uptake $M(t)$.

2. EXPERIMENTAL

2.1 Materials

Fibres: Three variants of Twaron® 1055 aramid fibres supplied by Akzo Nobel Central Research (Arnhem, The Netherlands) were used: HM, the as-spun fibre with no finish or surface activation; HMA, exhibiting an activated surface after treatment with glycerol glycidyl ether and piperazine; HMF, containing a surface finish (polyalkylene glycol). The exact details of the fibre surface treatments are proprietary, although some details have been given elsewhere [5]. The PBO fibre is a heat-treated high modulus (HM) Zylon® supplied by Toyobo Co. Ltd, Japan with a standard surface treatment. The M5 fibre is an experimental grade also heat treated and supplied by AKZO Nobel Central Research, Arnhem, The Netherlands.

Matrix: **A** two-part, cold curing epoxy resin consisting of LY5052 resin cured by HY5052 hardener at the ambient temperature for 7 days. Full details have been given [6].

Composites: Two specimen configurations were used: the 'Diffusion slab' (DS) type with a fibre fully embedded in the bulk of the matrix and the 'Double fibre pull-out' (DFPO) type with fibre ends exiting the matrix casting. In the DS specimen, the fibre can be reached by water vapour whereas the DFPO configuration facilitates a direct contact of a penetrant with the fibre and allows a different concentration profile to develop along the fibre. Both specimen types were fabricated in silicone moulds [7] to the typical dimensions a = 4.4 cm, b = 0.9 cm, h = 0.3 cm for the DS specimens and a = 0.6 cm, b = 0.5 cm, h = 0.3 cm for the DFPO specimens. Fibre depths $z(f)$ from the nearest flat surface were between 0.023 and 0.088 cm. Typically, three specimens in either configuration were used to investigate a particular fibre type.

Exposure: Composites were immersed in distilled water at the constant temperature of 22 ± 2 °C. As customary when investigating an ageing process, exposure times were incremented with the logarithm of time. The longest exposure times exceed 600 days.

Gravimetry: The weight $W(0)$ of a sample prior an exposure and all consecutive weights $W(t)$ after an exposure time, t, are determined by means of an analytical, electronic balance with the accuracy ± 0.00032 g. Working with exposed specimens, water is wiped off using an adsorbent paper before weighing.

Raman spectroscopy: Two microprobe systems, a Spex 1000M single monochromator and a Renishaw 1000 have been used. In the case of the former (Spex), a 15mW He-Ne laser with the wavelength of 632.8 nm was used as the incident radiation source with an intensity of 0.7 mW at the specimen and an exposure time of between 1 and 3 s. In the case of the latter (Renishaw), the 633 nm red line of a 28 mW He-Ne laser (model 127-25 Spectra Physics) is focused to give a power of about 2 mW at the fibre surface. For both systems, the scattered light is focused onto a sensitive charged-coupled device (CCD) camera interfaced with computers that control the spectrometer position and record the Raman spectra. Specimens

were placed on the stage of an Olympus BH-2 optical microscope connected to the monochromator and a 50× magnification objective lens to focus the laser beam polarised along the fibre axis to produce approximately 2 μm diameter spot on a fibre surface. Concerning the wave numbers used to investigate the fibres, the 1610 cm^{-1} peak for Twaron, 1618 cm^{-1} for PBO and 1507 cm^{-1} for M5 are used. The sensitivity factors $d\Delta\nu/d\varepsilon_f$ allowing the Raman band shift to be converted to fibre strain is set to 4.1 cm^{-1}/% for Twaron, 8.96 cm^{-1}/% for PBO and 14.56 cm^{-1}/% for the M5 fibre [8].

3. THEORETICAL BACKGROUND

With all explicit equations relevant for the analysis already given [1] and a separate study [9] dedicated to quantification of the principal characteristics D = 2.07 cm^2/sec and $M(\infty)$ = 6.8% of the diffusion process, it suffices to state that:

a) The uptake M(t) is readily derived for a specimen of any dimensions *a*, *b* and *h* as a fraction of the equilibrium saturation $M(\infty)$

$$M(t) = M(\infty)\left[1 - m\left(D, t, a, b, h\right)\right] \tag{1}$$

by generating the master curves $0 < m(D, t, a, b, h) < 1$ for each specimen and all exposure times at which determinations have been made. This is achieved by piecing together and overlapping outcome of two equations explicitly given in [2].

b) The reference mid-fibre strain ε_0 defines the fibre strain profile at the beginning of an exposure. It is obtained as the intercept of the dependence of the mid-fibre strain – including the value $\varepsilon(x=0,t=0)$ – on the square root of time:

$$\varepsilon(x=0,t) = \varepsilon_0 + S_\varepsilon\sqrt{t} \tag{2}$$

c) Concerning the Raman strain profiles, the shear-lag theory prescribes the strain distribution along a fibre embedded in a hygroscopic matrix exposed to moisture for a period of time, *t*, and with the mid-fibre strain attaining the value of $\varepsilon(x=0,t)$ as:

$$\varepsilon(x,t) = \varepsilon(x=0,t)\frac{\cosh(ns)}{\cosh(ns)-1}\left[1 - \frac{\cosh(nx/r)}{\cosh(ns)}\right] \tag{3}$$

where *n* is the Raman shear-lag parameter depending on the tensile modulus of a fiber of a length, *L* and the shear modulus of a matrix, *r* is the fiber radius and $s = L/(2r)$. Pragmatically, the Raman shear parameter *n* may be seen to be a ‘damage’ parameter that characterizes the state of an interface: A high value signals an efficient interface, any decay in *n* then reflects interface deterioration with $n(t)\rightarrow 0$ leading to $L_d(t)>0$.

d) The ‘swelling coefficient’ β relates the mid-fibre strain to the water uptake $M(t)$ and thus provides a link between the gravimetry and the Raman spectroscopy:

$$\varepsilon(x=0,t) - \varepsilon_0 = \beta_1 * M(t)\left[1 + \beta_2 * M(t)\right] \tag{4}$$

4. RESULTS & DISCUSSION

4.1 Water uptake

The values $D = 2.07\text{x}10^{-10}$ cm^2/s and $M(\infty) = 0.068$ as determined by investigating plain resin specimens [9] are used to predict water uptake of DS and DFPO model composites containing Twaron, PBO and M5 fibres. Fig. 1 compares experimental data with predictions. The fit is far from perfect, however the diffusion characteristics used appear to be an acceptable representation as the experimental data straddle theoretical dependencies. The ingress of water into the DFPO specimens is clearly seen to be a faster process than that into DS geometry. This is because the more cube-like geometry of the DFPO configuration has a smaller surface-to-volume ratio. As the matrix exclusively governs the moisture uptake, correlations are influenced neither by the fibre type nor by the surface treatment.

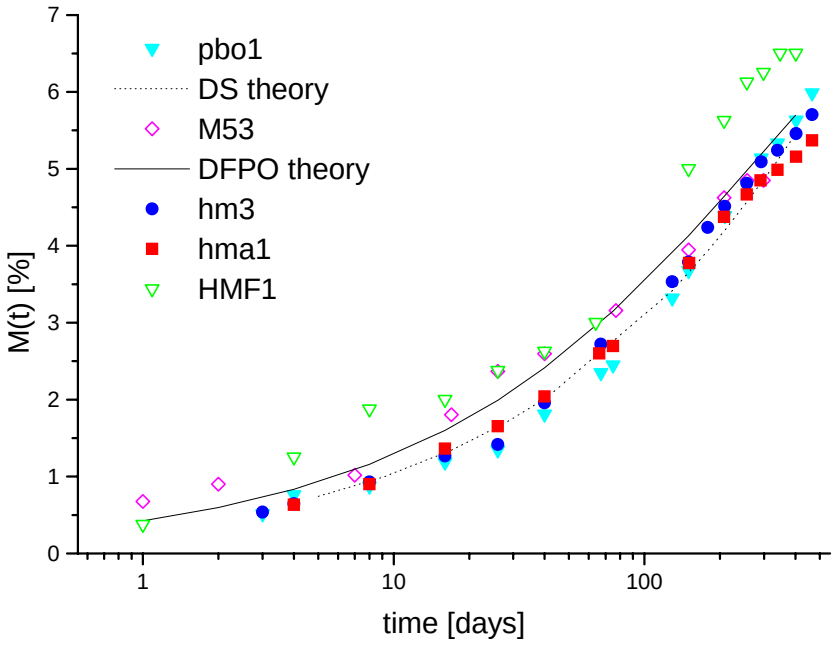

Fig. 1. Experimental (points) and theoretical (lines) dependencies of the moisture uptake for both specimen configurations: DS (filled-in symbols, small letters) and DFPO (open symbols, capital letters).

4.2 Raman strain profiles

The development of the Raman strain profiles for a DS specimen with the exposure time is illustrated in Fig. 2. The horizontal profile $\varepsilon(x,t=0) \approx 0$ measured prior any exposure rises with the time as the matrix absorbs water, swells and strains the fibre. The profiles exhibit a broad plateau in the mid-fibre region that allows the mid-fibre strain $\varepsilon(x=0,t)$ to be established. Near to the fibre ends, i.e. in the region $x \rightarrow |L/2|$, the profiles fall abruptly to zero. As the time progresses and a specimen absorbs more moisture, the area encompassed by the strain profile grows due to mid-fibre strain continuously rising. This is true as long as the fibre/matrix interface remains intact (e.g. for at least 179 days exposure as shown in Fig. 2). Debonding, however, observed for some fibres at longer exposure times changes the $\varepsilon(x,t)$ profile as shown for the exposure time of 289 days. A debond of length L_d manifested by a linear dependence of $\varepsilon(x,t)$ on x suddenly develops at this time and reduces the length of fibre over which stress is transferred from the matrix to fibre by a shear-lag process. This also upsets the development of $\varepsilon(x=0,t)$ with time.

Development of the Raman strain profiles for the DFPO specimen (not illustrated) is more complicated. Again the mid-fibre strain is an increasing function of time when a model composite remains intact. For this specimen type however, the mid-fibre strain $\varepsilon(x=0,t)$ values are not the highest values encountered as very pronounced maxima occur near the fibre ends. These maxima are particularly obvious at shorter exposure times. As the exposure time is increased the maxima become less prominent gradually converging to give strain distributions similar to those exhibited by the DS configuration (e.g. Fig. 2). The existence of these maxima near the fibre ends for the DFPO specimen is a result of three-dimensional Fickian ingress into a small rectangular specimen with the fibre position characterised by $y = 0$ and $z(f) \rightarrow |h/2|$ and the fibre strain monitored in the x-direction. The possibility of modelling this behaviour adequately has been demonstrated [1].

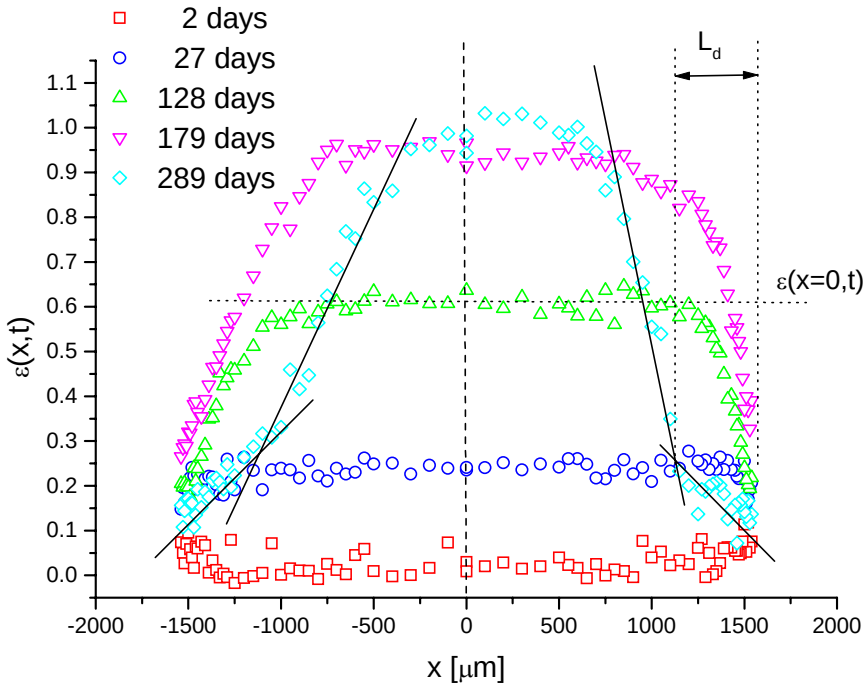

Fig. 2. Illustration of Raman strain profiles at selected exposure times for DS specimen (sample hm1).

4.3 Time dependence of the Raman shear-lag parameter *n*(t):

The Raman shear-lag parameter n has been determined for DS specimens and all exposure times prior debonding by iterating the value that yields the minimum of the sum of the squares of differences between experimental $\varepsilon(x,t)$ values and those predicted, for a given value of the mid-fibre strain fibre strain, by Eq. 3. Fig. 3. illustrates the $n(t)$ time dependence for the DS specimens containing the Twaron HMA fibre. An appreciable experimental scatter is noticeable and this is likely a consequence of deriving the micromechanical parameter from a structural response. Grouping all the data obtained for four individual HMA specimens and subjecting also the HM, HMF and PBO fibres to the same treatment, an exponential fit of the type

$$n(t) = P_1 * \exp\{-P_2 t\} \qquad (5)$$

has been applied resulting in the P_1 and P_2 parameters given in Table 1. On the basis of their mean values the HMA fibre appears to be associated with the strongest interface that has not

been breached by hygrothermal ageing. The PBO fibre is its opposite as it suffers from the fastest decay in $n(t)$. The surface finish applied to the HMF fibre might have a beneficial effect on the pristine interface but the gain is lost during the ageing process and the fibre treatment has to be concluded to have detrimental effect on composite durability. The HM fibre is characterised by similar P_1 and P_2 values as those for the HMA fibre, however the standard deviation on P_2 is more than twice larger.

Table I does not quote any P_1 and P_2 parameters for the M5 fibre. This is because the decay in $n(t)$ clearly (cf. Fig. 3) does not follow the exponential function. After an initial drop – co-measurable with the reduction observed for the PBO fibre within $150 > t > 0$ days – the $n(t)$ dependence levels off to a constant $n(t) \approx 0.015 \pm 0.005$ level at longer exposure time without any indication of debonding.

Table 1. Parameters P_1 and P_2 describing decay in the shear-lag parameter with time.

Fibre	Mean P_1	St. dev. P_1 [% mean]	Mean P_2 [day^{-1}]	St. dev. P_2 [% mean]
HM	0.1128	18	0.0047	31
HMA	0.1136	9	0.0044	12
HMF	0.1955	16	0.0055	32
PBO	0.1827	13	0.0165	17
M5	NA		NA	

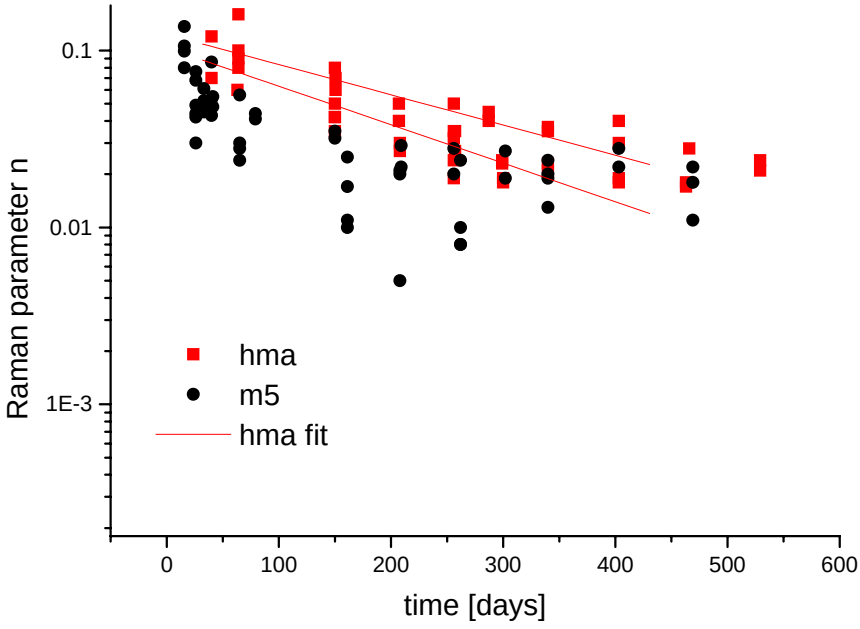

Fig. 3. Decay in the Raman shear-lag parameter n for the HMA and M5 fibres.

4.4 Debond evolution with time

The discussion of the decay in $n(t)$ is closely associated with the time dependence of the debond length, L_d as the debond onset is likely to be associated with $n \rightarrow 0$. The time dependence of experimentally-established debond lengths for the model composites of both

types is shown in Fig. 4. Both fibre ends are treated separately and the L_d values are normalised by the half-length $L/2$ of the original fibre. Debonding is never observed for composites containing the HMA and M5 fibres regardless of the specimen type. The others debond with DFPO specimens being more prone to debonding that the DS type. This indicates that the direct contact of a reinforcing fibre with the liquid water might represent an ageing regime more severe than that associated with the ingress of water vapour. Data in Fig. 4 are again scattered and $L_d(t)$ dependencies for a given specimen usually do not increase monotonically with time. Often one fibre end propagates debond to $L_d \rightarrow L/2$, whilst the other remains intact. Probably effects other than a shear transfer along a perfect cylinder influence the overall picture and 'an anchoring action' of fibre ends damaged during cutting might play a role.

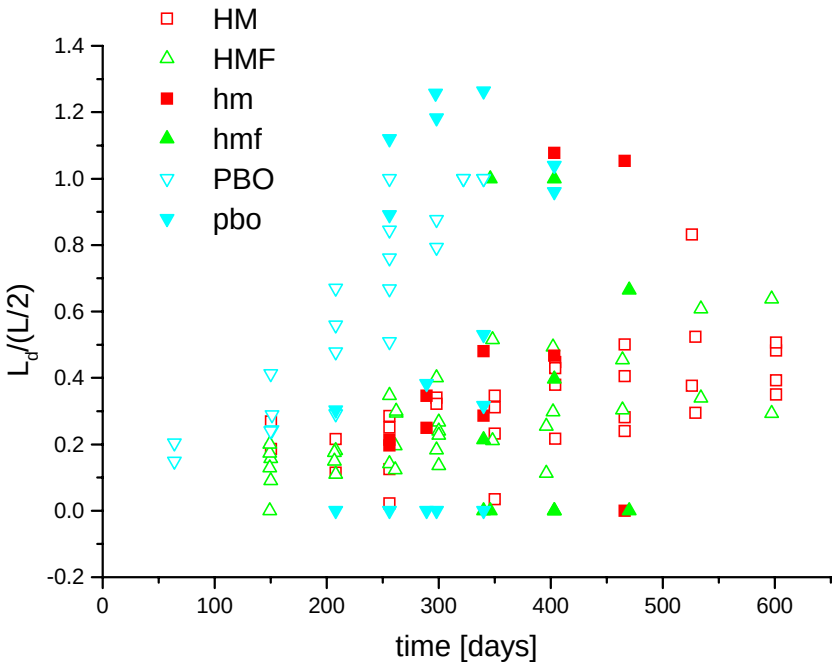

Fig. 4. Debond evolution with the exposure time for both specimen configurations: DS (filled-in symbols, small letters) and DFPO (open symbols, capital letters).

4.5 Dependence of the corrected mid-fibre strain on moisture uptake

Firstly, we correlate (Fig. 5) the corrected mid-fibre strain values $\varepsilon(x=0,t)$ - ε_0 with the moisture uptake $M(t)$ for the DS specimens containing Twaron (HMA, HM and HMF) fibres. The surface treatment is not seen to have any influence on the correlation. Secondly, we group all data obtained for the HM, HMA and HMF fibres into one population and carry out two theoretical fits using Eq. 4 setting the $\beta\{M(t)\}$ either as a linear ($\beta_1 \neq 0$, $\beta_2 = 0$) or quadratic ($\beta_1 \neq 0$, $\beta_2 \neq 0$) function of the moisture uptake. The former results in $\beta_1 = 0.2271 \pm 0.0037$, the latter in $\beta_1 = 0.1745 \pm 0.0121$ and $\beta_2 = 0.0777 \pm 0.0229$. The non-linear fit appears to be better as its χ^2 parameter is 50% lower than that obtained for the linear fit. A non-linear form of the β-function is thus offered to describe swelling of our epoxy matrix due to moisture absorption. Thirdly, the non-linear $\beta\{M(t)\}$ dependence is seen (Fig. 5) also to represents the behaviour of DFPO specimens.

Concerning the swelling behaviour of the DFPO model composites containing the PBO and M5 fibres, scattered $\varepsilon(x=0,t)$ - ε_0 versus $M(t)$ data do not signal any difference between these

two fibres and roughly follow the β{*M*(*t*)} function established for Twaron. The data are seen, nevertheless more scattered and lie below the narrow band typifying Twaron composites. The situation for the DS specimens is more complex (Fig. 6) with the PBO and M5 fibres exhibiting different behaviour: Whilst the PBO fibre appears to conform to the prediction made for Twaron, the M5 fibre is associated with a faster mid-fibre strain build up at lower moisture uptakes followed by a gradual convergence to a constant value at high moisture contents. This plateau appears to be more than 50% lower than the equilibrium ε(*x*=0,*t*=∞) = 1.68 % determined [10] for Twaron.

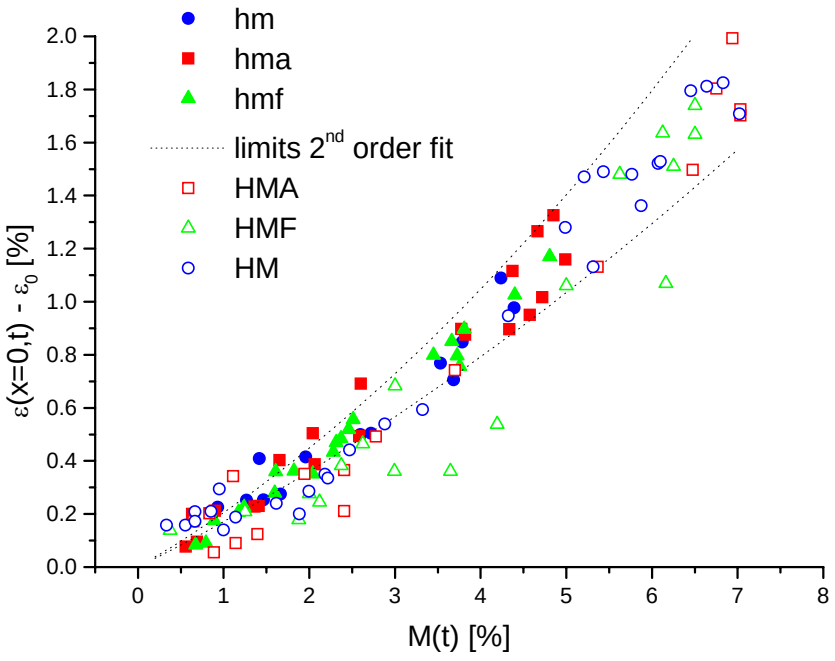

Fig. 5. Dependence of the corrected mid-fibre strain on the water uptake for composites containing Twaron fibres: DS (filled-in symbols, small letters) and DFPO (open symbols, capital letters).

4.6 Behaviour of the M5 fibre in relation to its chemical structure

The M5 fibre has been found to differ from PBO and Twaron in the following aspects: a) absence of any debonding in the DS and DFPO specimens (Fig. 4), b) levelling of the Raman shear-lag parameter, *n* for the DS specimen type (Fig. 3) and c) the mid-fibre strain converging to a constant value at high moisture uptake levels for the DS specimen type (Fig. 6).

Our findings are in line with a strong affinity of the polymer to water with its water regain reported to be 3.3× higher than for the PBO fibre. This is consistent with its structure – the polarity of the repeating unit that contributes towards a stronger fibre/matrix adhesion and strongly developed intramolecular hydrogen bonding. It is likely that the polymer structure of M5 changes drastically in presence of water. The intramolecular hydrogen bonding will probably collapse due to formation of intermolecular bonds between the water molecules and the polymer. Consequently, the fibre will swell in both the longitudinal and transverse direction. The transverse swelling is visualised to generate compressive radial stresses in the fibre/matrix interface region. If these exceed shear stresses near the fibre ends, the interface is very difficult to breach and debond cannot develop. Thus the Raman shear-lag parameter can be determined for very long exposure times and converges to low values never observed for

the Twaron fibres – HMF and HM – which do debond. The longitudinal swelling of the M5 fibre can then account for the mid-fibre strain convergence to the plateau level as the fibre straining due to matrix swelling being offset by the fibre swelling in the matrix cavity of a given size.

Regarding DFPO specimens containing the M5 fibre, their departure from the behaviour of the same specimens containing a Twaron fibre is less pronounced as this specimen construction restrains a fibre to a lesser degree.

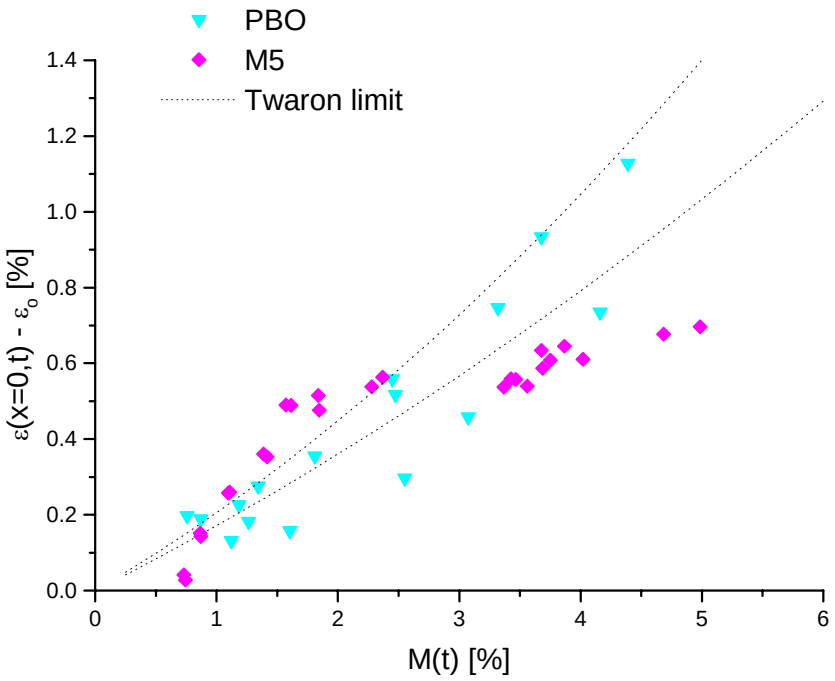

Fig. 6. Dependence of the corrected mid-fibre strain on the water uptake for the DS composites containing PBO and M5 fibres.

5. CONCLUSIONS

Moisture uptake is affected neither by the fibre type nor by the surface treatment. It can be modelled for both specimens type by means of diffusion characteristics determined for the resin castings.

Surface treatment applied to the Twaron fibre has been found to affect ageing of its interface in the epoxy matrix:

- The fibre with activated surface, HMA, has been found to be most resilient to hygrothermal ageing as it never debonds during exposures exceeding 600 days and its parameter P_2 that characterises decay of the Raman shear lag parameter n with time is low.
- The surface finish of the fibre HMF seems to improve the pristine interface. When subjected to hygrothermal ageing, however, the interface deteriorates (high value of P_2) and the fibre debonds at early stages of ageing.
- The behaviour of the untreated fibre HM is encompassed by those of the HMA and HMA.

The PBO and M5 fibres are very different from Twaron HMA:

- The PBO/epoxy interface has been found to be least robust
- Ageing of the M5/epoxy interface is not described by a simple exponential function as the Raman shear-lag parameter $n(t)$ converges to a plateau for long exposure times.

The DFPO specimen type is associated with an earlier debonding than the DS type.

The relationship between mid-fibre strain and moisture uptake satisfied by all fibres studied and the two specimen types used – with the exception of the M5 fibre in the DS specimens – is non linear: $\beta\{M(t)\} = 0.1745M(t)[1+0.0777M(t)]$.

Swelling of the M5 fibre in both the longitudinal and transverse direction due to disruption of intramolecular hydrogen bonding is offered as an explanation for this deviation.

ACKNOWLEDGEMENTS

The Institute for the Promotion of teaching Science, Thailand is thanked for financial support of Miss Ketsiri Kueseng during her PhD course. The overall programme of research was supported by grants from the EPRSC.

REFERENCES

1. **Cervenka, A.J., Young, R.J.** and **Kueseng, K.**, "Investigation of hygrothermal ageing phenomena in model composites by Raman spectroscopy", *Plastics, Rubber and Composites.*, **32** (2003), 206-214.
2. **Aronhime, M.T., Neumann, S.** and **Marom G.**, "The anisotropic diffusion of water in Kevlar-epoxy composites", *J. Mater. Sci.* **22** (1987), 2435-2446.
3. Toyobo Co. Ltd, Zylon® data sheet, Japan, 1996.
4. **van der Jagt, O.C.** and **Beukers A.**, "The potential of a new rigid-rod polymer fibre ('M5') in advanced composite structures", *Polymer.* **40** (1999), 1035-1044.
5. **Andrews, M.C. Bannister D.J.** and **Young R.J.**, "Review – The interfacial behaviour of aramid/epoxy model composites", *J. Mater Sci.* **31** (1996), 3893-3913.
6. **Cervenka A.J.**, **Bannister D.J.** and **Young R.J.,** "moisture absorption and interfacial failure in aramid/ epoxy composites", *Composites, Part A,* **29A**, (1998), 1137-1144.
7. **Bannister D.J.**, "Micromechanical and hygrothermal behaviour of a single-fibre epoxy resin composites", *PhD Thesis.* UMIST, October 1996.
8. **Kueseng K.**, "Hygrothermal effects on composite micromechanics", *PhD Thesis.* UMIST , September 2001.
9. **Cervenka, A.J., Young, R.J.** and **Kueseng, K.**, "Gravimetric determination of the diffusion characteristics of polymers using small specimens", *J. Polymer Sci*, (accepted for publication)
10. **Cervenka, A.J., Young, R.J.** and **Kueseng, K.**, "Micromechanical phenomena during hygrothermal ageing of model composites by Raman spectroscopy. Part I: Twaron fibres with different surface treatments", (to be published).